Eur. Phys. J. D **10**, 319–325 (2000)

THE EUROPEAN PHYSICAL JOURNAL D

EDP Sciences
© Società Italiana di Fisica
Springer-Verlag 2000

Strong potential second Born theory for low-energy electron emission in asymmetric collisions

D.H. Jakubaßa-Amundsen[a]

Institut für Kernphysik, University of Frankfurt, 60486 Frankfurt, Germany

Received 25 May 1999 and Received in final form 25 August 1999

Abstract. The ejection of low-energy target electrons by heavy projectiles is calculated in a second Born approximation, allowing for propagation of the electrons in the strong projectile field. For neutral projectile impact this theory provides a satisfactory description of the collision process down to quite low impact velocities. This is shown by comparing the theory with experimental electron spectra from 0.1 MeV/amu Ne^0 on He. However, when the projectile is charged the influence of its potential on the electronic final state may only be neglected for ejection of very low-energy electrons into the backward direction.

PACS. 34.50.Fa Electronic excitation and ionization of atoms (including beam-foil excitation and ionization)

1 Introduction

Studies of doubly differential cross-sections for electron emission from energetic ion-atom or atom-atom collisions provide a deep insight into the ionisation process. An exact theoretical description has to take into account the interaction of the active electron with the ionic/atomic field of both the projectile and the target not only in the intermediate state but also in the outgoing channel. However, theoretical models usually rely on some approximations to make the calculations feasible. Consideration as to whether the interaction of the electron with the projectile or with the target is dominant depends on the energy and direction of the ejected electron as well as on the nuclear charge of the collision partners. The soundness of such kinds of approximation must eventually be established by means of comparing the results with the measured electron spectra.

Early experiments with protons [1] were followed by systematic investigations with highly charged projectiles. The idea behind experiments using strong perturbing fields was that the simultaneous action of both the projectile and the target field, the so-called "two-center effects", could manifest themselves in the measured electronic momentum distributions. Such two-center effects were initially investigated for very fast bare ions ranging from C^{6+} to Ar^{18+} colliding with helium [2–4] as well as for very slow (≤ 0.1 MeV/amu) H^+ and He^{2+} projectiles impinging on He and Ne [5,6], followed by experiments using bare ions in the intermediate energy range down to 1 MeV/amu [7,8]. Subsequently systematic studies with partly stripped projectiles at 0.5 MeV/amu were made [9] in order to investigate the effect of additional projectile electrons on the ejected electron spectra.

Measurements of doubly differential cross-sections from neutral projectile impact, covering the whole range of electron momenta, are scarce and have basically been restricted to H^0 and He^0 projectiles [10,11]. However, experiments with 0.1 MeV/amu Ne^0 projectiles have now become possible due to a refined experimental technique allowing for an effective pick-up of electrons by the accelerated Ne^+ ion [12].

Unfortunately, even for the simplest collision system, A^{Z+} on H^0 [1,13], there is no theory available which provides an accurate description of the three-body break-up at all momenta of the ejected electron. The only quantum mechanical theory which gives satisfactory agreement with experiment at arbitrary energies and angles is the continuum distorted wave approximation in its eikonal initial state form (CDW-EIS [14,15]). This particular choice of initial state guarantees its correct normalisation [14] and moreover, CDW-EIS can be derived from the established channel-distorted two-center approximation [16] by means of a peaking approximation in the distortion factor [17]. It is also noteworthy that for short-range projectile fields, CDW-EIS is identical to the fully peaked strong potential second Born (SB2) theory [18–20]. Whereas CDW-EIS takes fully account of the final-state interaction of the emitted electron with both the projectile and the target (being a first-order theory in the kinetic energy), in the SB2 theory the ejected electron is described by an eigenstate of the parent atom while in the intermediate state it propagates in the strong perturbation field. Due to the full peaking nature of CDW-EIS with respect

[a] *Also at:* Physics Section, University of Munich, 85748 Garching, Germany.
e-mail: doris.jaku@lrz.uni-muenchen.de

to SB2, CDW-EIS is not able to describe details in some limited momentum regions (*e.g.* at the cusp).

On the other hand various higher-order perturbative approaches in one of the electron-ion (atom) interaction potentials can be used in order to gain insight into the relative importance of these potentials in particular regions of the electronic momentum distribution [21]. For example it is known from electron-loss cusp investigations that the representation of the final electronic state as a continuum projectile eigenstate is crucial [22] – even in the case of slow collisions and very heavy targets where the SB2 theory provides a very good description of the cusp features [19].

The aim of this paper is to investigate the low-energy electrons from target ionisation which, if transformed into the projectile frame of reference, would give rise to just the same cusp structure as that known from electron loss. By restricting ourselves to light targets (H, He) and heavy projectiles (C, Ne) and applying the SB2 theory, we investigate to what extent a theory which describes an ejected target electron in terms of a target continuum eigenstate, but which allows the electron in its intermediate state to move fully under the influence of the strong projectile field, is able to describe the measured electron distribution. In the next section, a short account of the SB2 theory is given and results for 0.1 MeV/amu Ne^0 on He are compared with experimental data [12,23]. The modification of SB2 to the case of bare projectiles is given in Section 3, and calculations for 2.5 MeV/amu C^{6+} + H as well as for 5 MeV/amu C^{6+} + He are shown in comparison with measured angular and energy distributions [2,4,13]. The conclusion is drawn in Section 4. Atomic units ($\hbar = m = e = 1$) are used unless otherwise indicated.

2 SB2 theory for neutral projectiles

Most electrons which are ejected during atom-atom collisions have very low energy with respect to the parent atom reference frame. They manifest themselves in two peak structures in the spectra, the soft electron peak from target ionisation near and below 10 eV (at all angles), as well as the electron loss peak from projectile ionisation around $v^2/2$ (at the forward angles) where $\mathbf{v}$ is the collision velocity. Since the binding energies of the outermost electrons are much alike for most neutral atoms, the simultaneous ionisation of projectile and target also plays a role and has to be included in the calculations [24].

We concentrate first on the singly inelastic (SI) process for target ionisation where the projectile atom is unaffected. In the strong potential second Born theory the transition amplitude for transfering a bound target electron into a continuum target eigenstate with momentum $\mathbf{k}_\mathrm{f}$ is given by

$$a_\mathrm{fi}^\mathrm{SB2} \;=\; -\mathrm{i}\int \mathrm{d}t\;\langle\psi^\mathrm{T}_{\mathbf{k}_\mathrm{f}}|\; V_\mathrm{P} + V_\mathrm{P} G_\mathrm{P} V_\mathrm{P}\;|\,\psi_i^\mathrm{T}\rangle. \qquad (2.1)$$

In this expression, V_P and $G_\mathrm{P} = (\mathrm{i}\partial_t - T - V_\mathrm{P} + \mathrm{i}\epsilon)^{-1}$ are the projectile field and single-particle propagator, respectively [25] where T is the kinetic electron energy. The initial and final single-particle states in an effective target field are denoted by $\psi^\mathrm{T}_\mathrm{i}$ and $\psi^\mathrm{T}_{\mathbf{k}_\mathrm{f}}$. Introducing into (2.1) two complete sets of plane waves $|\,\mathbf{q}^\mathrm{P}\rangle$ and $|\,\mathbf{k}^\mathrm{P}\rangle$ with momenta $\mathbf{q}$ and $\mathbf{k}$ in the projectile frame of reference, and applying the standard on-shell approximation $(1 + G_\mathrm{P}V_\mathrm{P})\,|\,\mathbf{q}^\mathrm{P}\rangle \;=\; |\,\psi^\mathrm{P}_\mathbf{q}\rangle$, one obtains

$$a_\mathrm{fi}^\mathrm{SB2} \;=\; -\mathrm{i}\int \mathrm{d}t \int \mathrm{d}\mathbf{k}\;\mathrm{d}\mathbf{q}\;\langle\psi^\mathrm{T}_{\mathbf{k}_\mathrm{f}}|\,\mathbf{k}^\mathrm{P}\rangle \times \langle\mathbf{k}^\mathrm{P}|\;V_\mathrm{P}\;|\,\psi^\mathrm{P}_\mathbf{q}\rangle\;\langle\mathbf{q}^\mathrm{P}|\,\psi^\mathrm{T}_\mathrm{i}\rangle. \quad (2.2)$$

This expression can be rewritten in terms of the Fourier transforms $\varphi^\mathrm{T}_\mathrm{i}$ and $\varphi^\mathrm{T}_\mathrm{f}$ of the initial and final target eigenstates. Using the classical straight-line approximation for the internuclear trajectory, the time integral becomes trivial and the doubly differential cross-section for the ejection of electrons with energy $E_\mathrm{f} = k_\mathrm{f}^2/2$ into the solid angle $\mathrm{d}\Omega$ results in

$$\frac{\mathrm{d}^2\sigma^\mathrm{SB2}}{\mathrm{d}E_\mathrm{f}\mathrm{d}\Omega_\mathrm{f}} = N_\mathrm{e}\frac{(2\pi)^4 k_\mathrm{f}}{v}\int \mathrm{d}\mathbf{q}'\delta(E_\mathrm{f} - E_\mathrm{i} + \mathbf{q}'\mathbf{v})|M_\mathrm{fi}|^2$$
$$M_\mathrm{fi} := \int \mathrm{d}\mathbf{k}\varphi_\mathrm{f}^{*\mathrm{T}}(\mathbf{k}+\mathbf{v})\langle\mathbf{k}^\mathrm{P}|V_\mathrm{P}|\psi^\mathrm{P}_{\mathbf{q}'+\mathbf{k}}\rangle\varphi_\mathrm{i}^\mathrm{T}(\mathbf{q}'+\mathbf{k}+\mathbf{v}) \qquad (2.3)$$

where $\mathbf{q}' := \mathbf{q} - \mathbf{k}$ is substituted for $\mathbf{q}$, and N_e is the occupation number of the initial state with energy E_i. The further evaluation of (2.3) proceeds along the lines of the SB2 theory for electron loss described in [19]. In particular, the scattering matrix element in (2.3) is replaced by the on-shell scattering amplitude and a minor peaking approximation is made. This peaking approximation is based on the fact that $\varphi^\mathrm{T}_\mathrm{i}$ is strongly peaked at momentum zero, making it sensible to take the scattering matrix element outside the integral over the azimuthal angle of $\mathbf{k}$ in M_fi [19]. Since the projectile field is of short range, no singularities occur in the scattering matrix element. Together with the fact that even with this peaking approximation the scattering matrix element is subject to a fourfold integration which smoothens its momentum dependence, the peaking approximation is expected to have very little influence on the theoretical cross-sections.

More crucial is the approximation by the on-shell scattering amplitude. Like the peaking approximation, this on-shell approximation becomes exact for vanishing target binding energy $|E^\mathrm{T}_\mathrm{i}|$, hence is the better the larger the asymmetry between projectile and target. We have investigated the on-shell/off-shell difference in the much simpler case of a first-order theory for charge exchange to the continuum [26], and proved that it is a measure of the influence of the target field during the collision, hence less important, the larger the collision velocity. In the present case of direct ionisation where the target field is fully accounted for in the final state we expect the on-shell approximation to give reasonable results even at collision velocities down to the orbiting velocity of the active target electron.

Alternatively, the SB2 result for electron loss, $(\mathrm{d}^2\sigma/\mathrm{d}E_\mathrm{f}\mathrm{d}\Omega_\mathrm{f})^\mathrm{EL}$, from [19] can be taken over as it is,

provided one transforms into the projectile reference frame, interchanges projectile and target, and reverses the collision velocity

$$\frac{\mathrm{d}^2\sigma^{\mathrm{SB2}}}{\mathrm{d}E_\mathrm{f}\mathrm{d}\Omega_\mathrm{f}} = \frac{k'_\mathrm{f}}{k_\mathrm{f}}\left(\frac{\mathrm{d}^2\sigma}{\mathrm{d}E_\mathrm{f}\mathrm{d}\Omega_\mathrm{f}}\right)^{\mathrm{EL}}\Bigg|_{\mathbf{v}\to-\mathbf{v},\ \text{projectile}\rightleftharpoons\text{target}} \tag{2.4}$$

where $\mathbf{k}'_\mathrm{f} = \mathbf{k}_\mathrm{f} - \mathbf{v}$ is the electron momentum in the projectile reference frame. Reversion of $\mathbf{v}$ is done by replacing the projectile-frame emission angle ϑ'_f (the angle between $\mathbf{k}'_\mathrm{f}$ and $\mathbf{v}$) by $\pi - \vartheta'_\mathrm{f}$. Also, the momentum $\mathbf{k}'_\mathrm{f}$ in the electron loss theory is now interpreted as the observed electron momentum for target ionisation.

Simultaneously with the ejection of a target electron, projectile electrons are excited or ionised, the more so, the smaller their binding energy. As an estimate of this process the first-order Born approximation is applied,

$$a_\mathrm{fi}^{\mathrm{DI}} = -\mathrm{i}\int \mathrm{d}t\ \langle \phi_\mathrm{f}^\mathrm{P}\ \psi_{\mathbf{k}_\mathrm{f}}^\mathrm{T} \mid V_\mathrm{ee} \mid \psi_\mathrm{i}^\mathrm{T}\ \phi_\mathrm{i}^\mathrm{P}\rangle \tag{2.5}$$

where $\phi_\mathrm{i}^\mathrm{P}$ and $\phi_\mathrm{f}^\mathrm{P}$ are the bound and excited projectile (single-particle) eigenstates. Since the transition is mediated by the electron-electron interaction V_ee which allows for small momentum transfers only, (2.5) accounts well for the doubly inelastic (DI) process as long as the energy of the observed electron is small. However, at larger energies (typically $\gtrsim 30$ eV), particularly at backward emission angles, higher-order Born terms which allow for a coupling to one of the nuclear fields [19,34] will gain importance and should be included in an accurate description of the DI process.

When calculating the doubly differential DI cross-section, one has to sum over all projectile final states. Using the conventional closure approximation [27], one obtains [19]

$$\frac{\mathrm{d}^2\sigma^{\mathrm{DI}}}{\mathrm{d}E_\mathrm{f}\mathrm{d}\Omega_\mathrm{f}} = N_\mathrm{e}\frac{8k_\mathrm{f}}{v^2}\int_{q'_{\min}}^{\infty}\frac{\mathrm{d}q'}{q'^3}S_\mathrm{in}(q') \times \int_0^\pi \mathrm{d}\varphi'_q|\langle\psi_{\mathbf{k}_\mathrm{f}}^\mathrm{T}|\mathrm{e}^{\mathrm{i}\mathbf{q}'\mathbf{r}_\mathrm{T}}|\psi_\mathrm{i}^\mathrm{T}\rangle|^2 \tag{2.6}$$

with $q'_{\min} = (E_\mathrm{f}^\mathrm{T} - E_\mathrm{i}^\mathrm{T} + \overline{\Delta E}_\mathrm{fi})/v$ and $\cos\vartheta'_q = q'_{\min}/q'$. The mean excitation energy of the projectile electron is set to $\overline{\Delta E}_\mathrm{fi} = I^\mathrm{P} + k_\mathrm{f}^2/2$ where I^P is the binding energy of the outermost electron (0.794 a.u. for Ne^0). This choice of $\overline{\Delta E}_\mathrm{fi}$ provides for the test system $\mathrm{He}^+ + \mathrm{H}$ the best agreement with an explicitly calculated sum over the excited states of the perturber atom [27]. Variations of $\overline{\Delta E}_\mathrm{fi}$ could change the total cross-sections for target ionisation by some 20% (or even more at backward angles) in the cases of Figures 1 and 2. $S_\mathrm{in}(q')$ denotes the incoherent scattering form factor tabulated in [28].

In the actual calculations, Slater-screened hydrogenic wavefunctions to an effective charge $Z_\mathrm{eff} = 1.7$ were taken for the target, with an initial-state energy $E_\mathrm{i}^\mathrm{T} = -0.91795$ a.u. For Ne^0 the scattering amplitude was calculated from a partial wave analysis, using the following

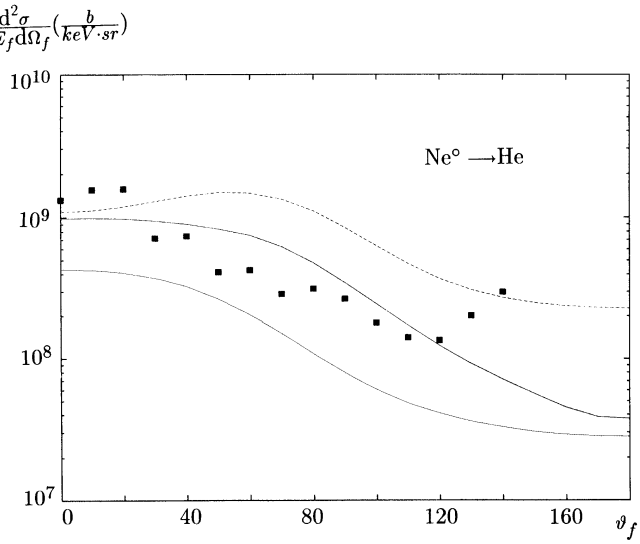

Fig. 1. Doubly differential cross-section for the emission of 20 eV electrons from 0.1 MeV/amu Ne^0 + He collisions (v = 2 a.u.) as a function of emission angle ϑ_f. The experimental data (■) are taken from Jalowy [23]. Theory: —— SB2, SI+DI; ····· DI (bottom curve); - - - - B1, SI+DI.

composition of the projectile field

$$V_\mathrm{P} = V_\mathrm{s} + V_\mathrm{pol} + V_\mathrm{ex} \tag{2.7}$$

where V_s is the static Hartree-Fock potential for the Ne atom (in a parametrised form [29]). For the polarisation field V_pol we have taken the parameter-free representation of Gianturco *et al.* [30] with the dipole polarisability α = 2.663 a.u. for Ne^0. The exchange field V_ex was chosen as the local modified semiclassical exchange (MSCE) potential [31]. However, exchange affects the results by 5–10% only.

In Figure 1 the angular distribution of 20 eV electrons emitted from collisions of 0.1 MeV Ne^0 on He is shown. Both singly inelastic and doubly inelastic contributions decrease smoothly with angle, DI gaining somewhat more importance at the backward angles. While the 0°/180° asymmetry of the first-order Born approximation is just due to the finite electron energy, the SB2 is truly asymmetric (also for $E_\mathrm{f} \to 0$) because as a higher-order theory it is sensitive to the phase of $\psi_{\mathbf{k}_\mathrm{f}}^\mathrm{T}$. Such a forward/backward asymmetry is well-known from electron loss cusp investigations [19]. However, the transformation (2.4) reverses the asymmetry such that now forward emission is enhanced. Comparison is made with experimental data from Jalowy and coworkers [12,23] which have an absolute uncertainty of ±40%. Apart from the backward rise in contrast to theory (which is presently not understood), the data can be explained by the SB2 model within a factor of 2. We have included in the figure results from a first-order Born (B1) calculation for both SI and DI processes (for the SI contribution, only the first term in (2.1) is retained, approximating V_P by V_s which is conventionally done in B1 calculations since the bound-state function $\psi_\mathrm{i}^\mathrm{T}$ cuts off the long-range tail of V_P (originating from V_pol) in the

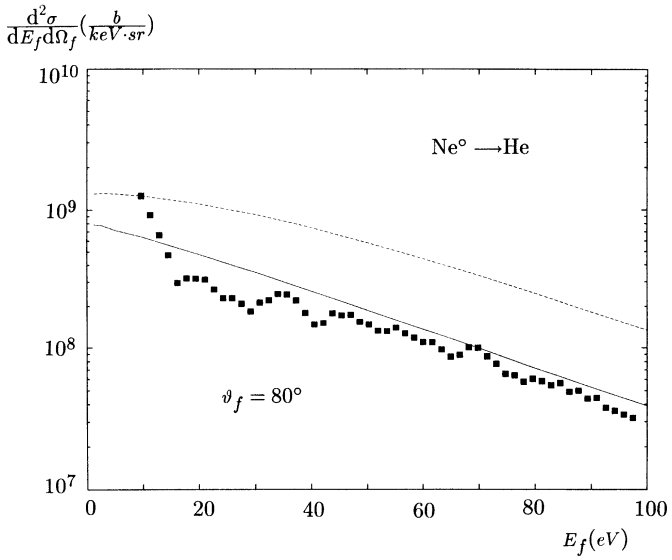

(a)

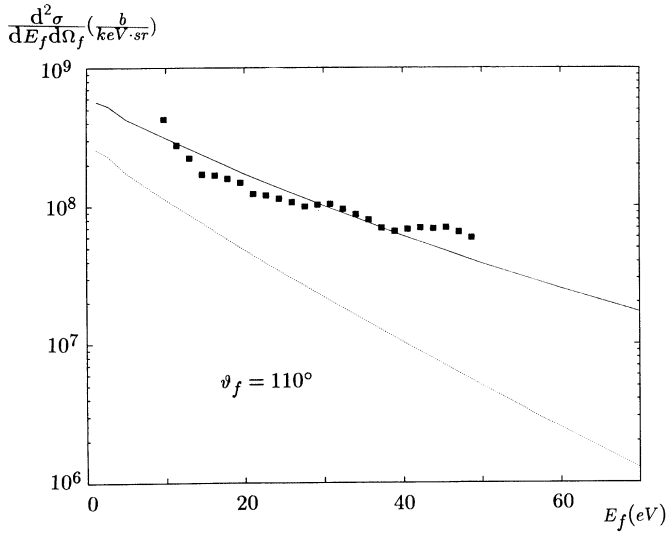

(b)

Fig. 2. Doubly differential cross-section for electron emission at angles 80° (a) and 110° (b) from 0.1 MeV/amu Ne^0 + He collisions as a function of electron energy E_f. The experimental data (■) are taken from Jalowy [23]. Theory: —— SB2, SI+DI; ····· DI; - - - - B1, SI+DI.

transition matrix element). These results overestimate the data, a fact well-known for ionisation in strong fields [32].

The SB2 theory as formulated above is only able to correctly describe the low-energy electrons from target ionisation. For example, it deteriorates for electrons of higher energies where electron loss peak or binary encounter peak phenomena come into play: electron loss is only included by means of the DI process where the final projectile states are integrated over. The binary encounter peak, on the other hand, is a two-body phenomenon which requires either free electron propagation or intermediate as well as final electronic motion in the strong potential. In order to test SB2 for the spectral distribution of the electrons, we have therefore restricted ourselves to the larger emission angles where none of these peak phenomena are present (the electron loss peak disappears for $\vartheta_f \gtrsim 30°$ due to the small collision velocity and the binary encounter peak fades out around 60° [23]).

Figure 2 shows the electron spectra for $\vartheta_f = 80°$ and 110°. The SB2 theory is seen to correctly reproduce the measured energy dependence up to quite high energies (50–100 eV), whereas the B1 theory provides a similar energy dependence but too high intensities (Fig. 2a). At small E_f, the (first-order) DI contribution (shown separately in Fig. 2b) provides about half the measured intensity, but decreases rapidly at the higher E_f. One should keep in mind that beyond 30 eV, the higher-order DI processes will start to push theory slightly upwards.

Below 20 eV, the experimental data are getting unreliable because electric and magnetic stray fields will influence the electron trajectories, but also because of inaccuracies in the absolute normalisation of the data [23].

3 SB2 theory for fully stripped projectiles

In the case of bare projectiles where the interaction V_P is purely Coulombic, formula (2.3) can be evaluated exactly without any further approximation. The scattering matrix element is given by [33]

$$\langle \mathbf{k}^P | V_P | \psi^P_{\mathbf{q}'+\mathbf{k}} \rangle = -\frac{Z_P}{2\pi^2} e^{\pi\eta_Q/2} \Gamma(1 - i\eta_Q) \times \frac{[k^2 - (Q + i\epsilon)^2]^{-i\eta_Q}}{(q'^2)^{1-i\eta_Q}} \tag{3.1}$$

with $\mathbf{Q} = \mathbf{q}' + \mathbf{k}, \eta_Q = Z_P/Q$ and $\epsilon \to 0$. It should be noted that the on-shell approximation from Section 2 must not be made here: while for short-range electron-projectile interactions the scattering matrix element coincides in the elastic limit ($Q = k$) with the elastic scattering amplitude, this is not the case for a $1/r$-potential. In particular, the peculiarities of the Coulomb field produce an extra phase which diverges at $Q = k$ (see Eq. (3.1)).

The choice of (effective) Coulomb states for the target electron [19] requires $\mathbf{k}$ to be substituted by $\mathbf{k}' := \mathbf{k}+\mathbf{v}-\mathbf{k}_f$ in order to cope with the singularities. One obtains

$$\frac{d^2\sigma}{dE_f d\Omega_f} = N_e \frac{8 Z_P^2 Z_T^3}{\pi^3 v} \frac{1}{1 - e^{-2\pi\eta_f}} \int \frac{d\mathbf{q}'}{q'^4} \delta(E_f - E_i^T + \mathbf{q}'\mathbf{v}) \times \left| \int d\mathbf{k}' \frac{(k'^2 + 2\mathbf{k}'\mathbf{k}_f - i\epsilon)^{-i\eta_f - 1}}{(k'^2)^{1-i\eta_f}} \varphi_i^T(\mathbf{Q} + \mathbf{v}) \times e^{\pi\eta_Q/2} \Gamma(1 - i\eta_Q)(q'^2 - 2\mathbf{q}'\mathbf{Q} - i\epsilon)^{-i\eta_Q} \right|^2 \tag{3.2}$$

where $\eta_f = Z_T/k_f$ with Z_T the (effective) target nuclear charge. For the further evaluation, spherical coordinates are introduced for $\mathbf{q}'$ and $\mathbf{k}'$ with the respective quantisation axes $\mathbf{v}$ and $\mathbf{k}_f$. Equation (3.2) then reduces

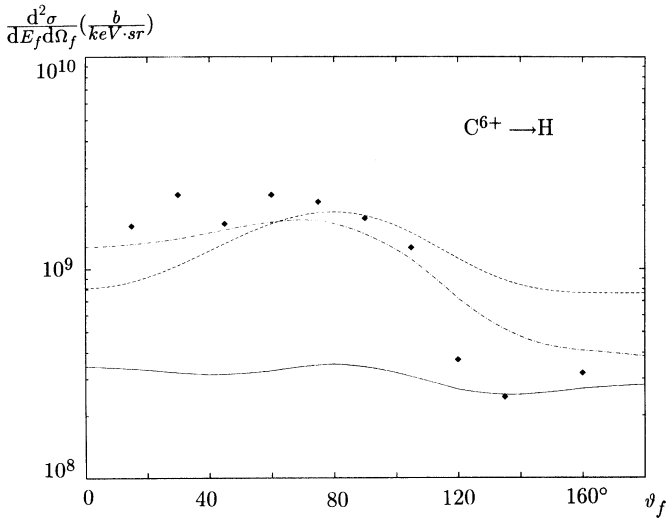

Fig. 3. Doubly differential cross-section for the emission of 5 eV electrons from 2.5 MeV/amu C^{6+} + H collisions (v = 10 a.u.) as a function of emission angle ϑ_f. The experimental data (♦) are taken from Tribedi *et al.* [13]. Theory: —— SB2; - - - - B1; – · – · – CDW-EIS (from [13]).

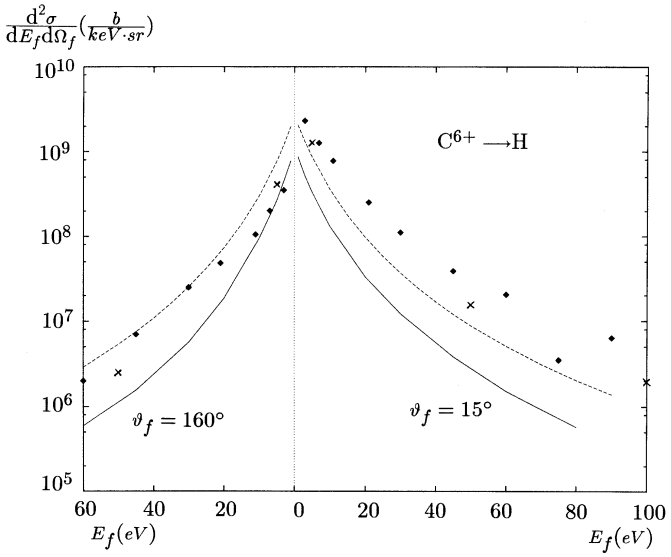

Fig. 4. Doubly differential cross-section for electron emission at angles 15° (right-hand abscissa) and 160° (left-hand abscissa) from 2.5 MeV/amu C^{6+} + H collisions as a function of electron energy E_f. The experimental data (♦) are those from Tribedi *et al.* [13]. Theory: —— SB2; - - - - B1; × × × CDW-EIS (from [13]).

to a five-fold integral which is evaluated numerically (note that the peaking approximation which is made in case of neutral projectiles would be poor because of the additional singularities in the integrand).

Figures 3 and 4 show results for the three-body system 2.5 MeV/amu C^{6+} colliding with atomic hydrogen where no approximations for the target wavefunction are needed. Comparison is made with the new experimental data from Tribedi and coworkers [13]. In contrast to neutral projectile impact, the angular distribution of the low-energy electrons (E_f = 5 eV, Fig. 3) cannot be explained by the SB2 model. The high experimental intensities for electron emission into the forward hemisphere clearly show the effect of the perturbing field on the electrons in their final state, which is supported by the CDW-EIS results. Only at angles beyond 120° does SB2 agree with the data, *i.e.* is it admissible to neglect the projectile final-state interaction for electrons with such a low velocity relative to the target. However, as seen in Figure 4 where the energy distribution at one forward and one backward emission angle is shown, SB2 falls below experiment with increasing electron energy (for $E_f \gtrsim 20$ eV) even at ϑ_f as large as 160°. Taken into consideration that at these higher energies, CDW-EIS is much closer to the data than SB2, we interpret this result in terms of an increasing influence of the projectile field on the outgoing electron with increasing electron velocity with respect to the target core. For the sake of comparison, results from the first-order Born theory are also shown in Figures 3 and 4, and this theory underestimates the experimental yields in forward direction, but overestimates them at large angles. However, since the Born series (as a perturbation series in terms of V_P) is divergent for strong projectile fields, there is not too much significance in these B1 results.

The strong influence of V_P on the outgoing electron in the forward hemisphere is not a peculiarity of the above three-particle system. This was verified by a series of calculations on the momentum distribution of low-energy electrons from bare ion impact (C^{6+}, O^{8+}, Ne^{10+}) on helium at various collision velocities (1–5 MeV/amu) according to experimental data from [2,4,8]. As a typical example, we show in Figure 5 the forward and backward electron spectra from 5 MeV/amu C^{6+} on He in comparison with the measurements from Schiwietz and coworkers [2]. The results are qualitatively the same as for the 2.5 MeV/amu C^{6+} + H system studied above.

4 Conclusion

We have applied the strong potential second Born approximation to the emission of low-energy target electrons during heavy atom and ion impact on light targets. By comparing SB2 and, where available, CDW-EIS results to experimental data doubly differential in electron energy and angle, we were able to sort out the importance of electron propagation in the projectile field, as well as the adequacy of the ejected electrons moving solely in the field of the target core.

In the case of neutral heavy atom impact where the perturbing potential is of short range, the SB2 theory gives a good account of the measurements. Hence, at all emission angles and for electron energies low enough to exclude electron loss peak or binary encounter peak features in the spectra, the influence of the projectile field has to be accounted for in the intermediate state of the electron, but can safely be neglected in its final state.

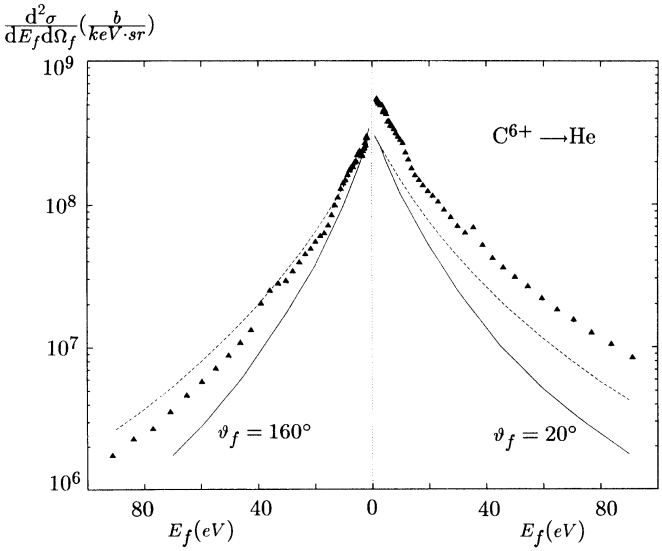

Fig. 5. Doubly differential cross-section for electron emission at angles 20° (right-hand abscissa) and 160° (left-hand abscissa) from 5 MeV/amu C^{6+} + He collisions ($v = 14.15$ a.u.) as a function of electron energy E_f. The experimental data (▲) are taken from Schiwietz *et al.* [2]. Theory: ——— SB2; - - - - B1.

This picture holds true down to quite low collision velocities ($v \gtrsim 2$ a.u.) where other higher-order perturbation theories are bound to fail. Our present findings are supported by previous SB2 results for the electron loss cusp [19,21] from He^+ on Ar, Xe collisions at $1.7 \lesssim v \lesssim 4$ a.u. The interpretation is, however, more direct for the low-energy target electrons since there is no strong influence of the detector resolution.

We have also demonstrated the importance of the simultaneous projectile and target ionisation when both collision partners are neutral. For small electron energies this process is of the same magnitude as target ionisation by an inert projectile at all angles. For larger energies the first-order Born theory for DI decreases strongly and higher-order terms not considered in the present calculations will come into play. That DI remains important, although perhaps to a lesser extent, can be inferred from calculations describing electron loss as charge transfer to the continuum [34].

The situation concerning the applicability of SB2 is different for highly stripped projectiles. In that case, the long range of the projectile field causes the slow electrons emitted into the forward hemisphere to move in the field of *both* the projectile and the target: neither field can be treated perturbatively. The influence of the projectile is to strongly increase the electron yield, as shown by the CDW-EIS results. In contrast, allowing for propagation in the projectile field with a subsequent "recapture" by the target (the SB2) leads to an unphysical reduction of the intensity. At backward angles and very small emission energies on the other hand, the target field dominates the outgoing electrons and the influence of the projectile field may be neglected: provided it is taken into account in the electronic intermediate state. In fact CDW-EIS overestimates the backward data slightly while SB2 does not. However, when the electron energy is increased such that the separation of the electron from the parent atom gets more efficient even at backward angles, the projectile field will again dominate the final state (the more so, the higher the projectile charge). We finally mention that at electron energies as high as $v^2/2$ or beyond, the outgoing electron can well be described by a pure projectile eigenstate, as demonstrated by application of a theory for charge transfer to the continuum to experiments on 0.5 MeV/amu B^{2+}–B^{5+} colliding with He [35]. Hence the studies with higher-order perturbative theories in one of the atomic potentials provide a valuable supplement to investigations within the CDW approach.

I am particularly grateful to P. Mokler and B. Fricke for supporting contacts with the physical community. I should also like to thank T. Jalowy for the excellent collaboration and for the access to his unpublished experimental data.

References

1. M.E. Rudd, J. Macek, Case Stud. At. Phys. **3**, 47 (1972).
2. G. Schiwietz, H. Platten, D. Schneider, T. Schneider, W. Zeitz, K. Musiol, R. Kowallik, N. Stolterfoht, HMI Report No. B447, Berlin (1987).
3. N. Stolterfoht, X. Husson, D. Lecler, R. Köhrbrück, B. Skogvall, S. Andriamonje, J.P. Grandin, *XVIIth ICPEAC Brisbane*, edited by I.E. McCarthy *et al.* (Griffith University Press, Brisbane, 1991), Abstracts of Contributed Papers, p. 393.
4. N. Stolterfoht, H. Platten, G. Schiwietz, D. Schneider, L. Gulyás, P.D. Fainstein, A. Salin, Phys. Rev. A **52**, 3796 (1995).
5. G.C. Bernardi, S. Suárez, P.D. Fainstein, C.R. Garibotti, W. Mecbach, P. Focke, Phys. Rev. A **40**, 6863 (1989).
6. S. Suárez, C. Garibotti, G. Bernardi, P. Focke, W. Mecbach, Phys. Rev. A **48**, 4339 (1993).
7. D.H. Lee, P. Richard, T.J.M. Zouros, J.M. Sanders, J.L. Shinpaugh, H. Hidmi, Phys. Rev. A **41**, 4816 (1990).
8. J.O.P. Pedersen, P. Hvelplund, A.G. Petersen, P.D. Fainstein, J. Phys. B **24**, 4001 (1991).
9. R.D. DuBois, L.H. Toburen, M.E. Middendorf, O. Jagutzki, Phys. Rev. A **49**, 350 (1994).
10. L. Sarkadi, J. Pálinkás, A. Kövér, D. Berényi, T. Vajnai, Phys. Rev. Lett. **62**, 527 (1989).
11. O. Heil, R.D. DuBois, R. Maier, M. Kuzel, K.O. Groeneveld, Z. Phys. D **21**, 235 (1991).
12. T. Jalowy, M. Kuzel, R. Wünsch, R. Neugebauer, D. Hofmann, L. Sarkadi, A. Báder, L. Víkor, G. Víkor, P. Focke, D.H. Jakubaßa-Amundsen, M.W. Lucas, G. Sigaud, K.O. Groeneveld, Nucl. Instrum. Meth. B **124**, 405 (1997).
13. L.C. Tribedi, P. Richard, W. DeHaven, L. Gulyás, M.W. Gealy, M.E. Rudd, J. Phys. B **31**, L369 (1998).
14. D.S.F. Crothers, J.F. McCann, J. Phys. B **16**, 3229 (1983).
15. P.D. Fainstein, V.H. Ponce, R.D. Rivarola, J. Phys. B **24**, 3091 (1991).
16. J.N. Madsen, K. Taulbjerg, J. Phys. B **28**, 1251 (1995).
17. J.N. Madsen, K. Taulbjerg, Phys. Scripta **T73**, 137 (1997).

18. H.M. Hartley, H.R.J. Walters, J. Phys. B **20**, 3811 (1987).
19. D.H. Jakubaßa-Amundsen, J. Phys. B **26**, 2853 (1993).
20. M.W. Lucas, D.H. Jakubaßa-Amundsen, M. Kuzel, K.O. Groeneveld, Int. J. Mod. Phys. A **12**, 305 (1997), Sect. 2.2.
21. D.H. Jakubaßa-Amundsen, Nucl. Instrum. Meth. B **86**, 82 (1994).
22. F. Drepper, J.S. Briggs, J. Phys. B **9**, 2063 (1976).
23. T. Jalowy, Diploma thesis, University of Frankfurt, 1997; and private communication.
24. D.R. Bates, G. Griffing, Proc. Phys. Soc. A **67**, 663 (1954).
25. C.J. Joachain, *Quantum Collision Theory* (Amsterdam, North Holland, 1983), p. 361.
26. T. Jalowy, D.H. Jakubaßa-Amundsen, M.W. Lucas, K.O. Groeneveld, to appear in Phys. Rev. A **61**, 22714 (2000).
27. M.H. Day, J. Phys. B **14**, 231 (1981).
28. D.T. Cromer, J.B. Mann, J. Chem. Phys. **47**, 1892 (1967).
29. T.G. Strand, R.A. Bonham, J. Chem. Phys. **40**, 1686 (1964).
30. F.A. Gianturco, K.T. Tang, J.P. Toennis, D. De Fazio, J.A. Rodriguez-Ruiz, Z. Phys. D **33**, 27 (1995).
31. F.A. Gianturco, S. Scialla, J. Phys. B **20**, 3171 (1987).
32. H.R.J. Walters, J. Phys. B **8**, L54 (1975).
33. H.A. Bethe, E.E. Salpeter, *Encyclopedia of Physics*, edited by S. Flügge (Berlin, Springer, 1957), Vol. 35, p. 126.
34. M. Kuzel, R.D. DuBois, R. Maier, O. Heil, D.H. Jakubaßa-Amundsen, M.W. Lucas, K.O. Groeneveld, J. Phys. B **27**, 1993 (1994).
35. D.H. Jakubaßa-Amundsen, Z. Phys. D **34**, 9 (1995).